

## Large $Q$ factor variation within dense, highly ordered Ba(Zn<sub>1/3</sub>Ta<sub>2/3</sub>)O<sub>3</sub> system

E. Koga<sup>a</sup>, Y. Yamagishi<sup>a</sup>, H. Moriwake<sup>b</sup>, K. Kakimoto<sup>c</sup>, H. Ohsato<sup>c,\*</sup>

<sup>a</sup> Department of Engineering, Panasonic Electronic Devices Hokkaido Co. Ltd., Chitose 066-8502, Japan

<sup>b</sup> Panasonic Electronic Devices Co. Ltd., Kadoma 571-8506, Japan

<sup>c</sup> Materials Science and Engineering, Nagoya Institute of Technology, Nagoya 466-8555, Japan

Available online 2 November 2005

### Abstract

The large amount of  $Q$  factor variation within dense, highly ordered region of Ba(Zn<sub>1/3</sub>Ta<sub>2/3</sub>)O<sub>3</sub> (BZT) system were studied by means of crystal structure analysis, micro-structural analysis and electrical measurements using samples around stoichiometric BZT. Presence of small amount of secondary phase (e.g., less than 1%) affects  $Q$  factor decrements even in the dense (density = 7.15–7.78 g/cm<sup>3</sup>), highly ordered (estimated ordering ratio around 70–80%) samples. This suggests that the structural order and the presence of the secondary phase are playing an important role on  $Q$  factor in BZT system. Therefore, suppressions of small amount of secondary phase (e.g., less than 1%) by strict composition control can provide further  $Q$  factor improvements. Single phase ordered perovskite obtained in the vicinity of stoichiometric BZT showed an improvement in  $Q$  factor ( $Q \times f = 133,000$  GHz) by extended sintering up to 400 h at 1400 °C.

© 2005 Elsevier Ltd. All rights reserved.

**Keywords:** Dielectric properties;  $Q$  factor; Perovskites; X-ray methods

### 1. Introduction

The complex perovskite type Ba(Zn<sub>1/3</sub>Ta<sub>2/3</sub>)O<sub>3</sub> (BZT) has an exceptionally high  $Q$  factor ( $Q \times f \approx 10 \times 10^4$  GHz) at microwave frequency, and has been used as dielectric resonator material for the mobile communication.<sup>1,2</sup> The complex perovskite with the general formula  $A(B_{1/3}^1B_{2/3}^2)O_3$  can form disordered or ordered phases. The driving force for the ordering has been explained in relation to the difference in ionic charges or ionic radii between  $B^1$  and  $B^2$ .<sup>3</sup> In the case of BZT, both ordered-type with a trigonal space group of  $P\bar{3}m1$  and disordered-type with a cubic phase space group of  $Pm\bar{3}m$  were formed, depending on the synthesis conditions.<sup>2</sup> By long-time sintering (e.g., around 100 h), the  $Q$  factor of BZT was improved with superlattice ordering enhancement.<sup>2</sup> Therefore, the structural order has been considered playing a crucial role in the  $Q$  factor improvement.<sup>2–5</sup> Quantitative analysis of the relationship between the  $Q$  factor and the ordering was reported by Koga and Moriwake.<sup>6</sup> The  $Q$  factor of BZT system was found to depend not only on the ordering but also on their ceramic microstructure. Recently, influences of composition deviation

from around BZT on superlattice ordering and microwave  $Q$  factor were reported by Koga et al.<sup>7</sup> The superlattice ordering ratio (ordered–disordered structure formation) was found to be dependent on the slight composition deviation around BZT. The ordered structure with perovskite single phase was obtained in vicinity of the stoichiometric BZT. In this region, a significant high  $Q$  factor of  $Q \times f = 110,000$  GHz was found. The disordered perovskite and the secondary phase in the ordered perovskite were thought to be the causes of  $Q$  factor decrements. Suppressions of the secondary phase and the disordered phase by strict composition control for further  $Q$  factor improvements of the BZT system were suggested.

Despite of these efforts, the detailed mechanism of high  $Q$  factor of this system has not been fully understood, namely, quite large amount of  $Q$  factor variation within dense, highly ordered single phase region of the BZT system. If we could understand the origin of this large amount of the  $Q$  factor variation, then we could suggest methods for further  $Q$  factor improvements of the BZT system.

In this paper, we performed precise secondary phase analysis by backscattered electron image (BEI) using scanning electron microscope (SEM) equipped with X-ray microanalyzer (XMA) and then discussed the relationship between the presence of the secondary phase and the  $Q$  factor improvements. Additionally,

\* Corresponding author.

the  $Q \times f$  improvement limit of the single phase ordered perovskite of this system by extended sintering was also studied.

## 2. Experimental procedure

All samples of the general formula  $x\text{BaO}-y(1/3\text{ZnO})-z(2/3\text{TaO}_{5/2})$  ( $x, y$  and  $z=0.97-1.03$ ,  $x+y+z=3.00$ ) were prepared by the conventional mixed-oxide reaction method and were sintered at  $1400^\circ\text{C}$  for 100 h in air. Additionally, for some samples extended sintering was performed up to 400 h. The crystal structure of the sintered ceramics was examined by powder XRD and Rietveld analysis using Rietan 2000.<sup>8</sup> Details on the synthesis conditions and on the XRD analysis are given elsewhere.<sup>7</sup> The microstructure were observed by BEI using the well-polished samples. Quantitative analyses of the

contents of the secondary phases were done using BEI photograph ( $\times 1.0\text{k}$ , area of  $100\ \mu\text{m} \times 120\ \mu\text{m}$ ). The contents of the secondary phases were estimated from the area ratio of the secondary phase to the matrix phase, excluding the area of the pore region. The dielectric properties were measured at 4–6 GHz using a network analyzer. Dielectric constant was measured by Hakki and Coleman's method.<sup>9</sup>  $Q$  factor was determined by resonant cavity method using the  $\text{TE}_{01\delta}$  mode.

## 3. Results and discussion

### 3.1. Precise secondary phase analysis by backscattered electron image

Fig. 1 shows BEI photograph of each sample. Assuming that the secondary phase has different composition from the

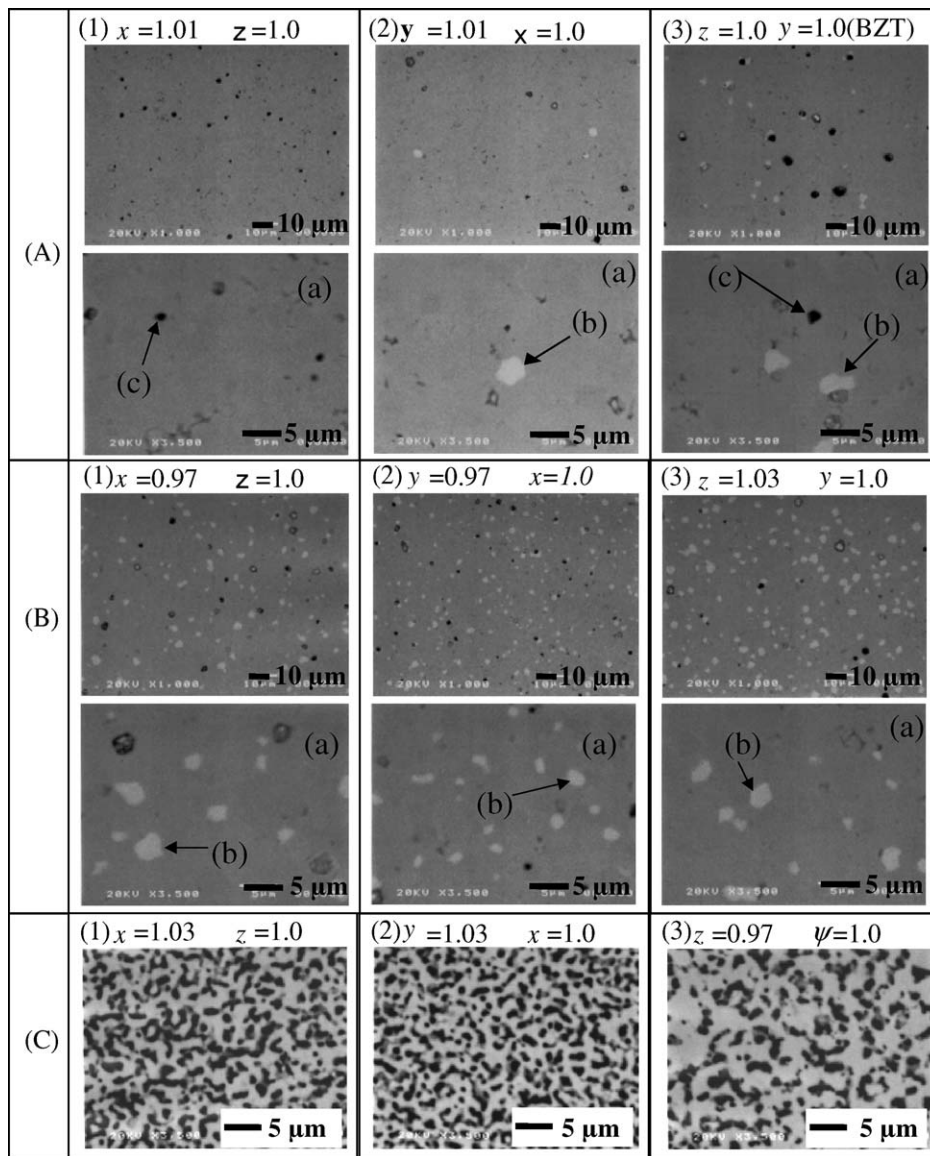


Fig. 1. Polished surface backscattered electron image of  $x\text{BaO}-y(1/3\text{ZnO})-z(2/3\text{TaO}_{5/2})$  ( $x+y+z=3.0$ ), (a) the matrix phase (gray), (b) the secondary phase (white) and (c) the pore (black): S shows the contents of secondary phase detected by BEI. (A) Ordered perovskite with secondary phase not detected by XRD: (1)  $S=0.0\%$ , (2)  $S=0.2\%$  and (3)  $S=0.8\%$ ; (B) ordered perovskite with secondary phase detected by XRD: (1)  $S=6.7\%$ , (2)  $S=2.5\%$  and (3)  $S=4.0\%$ ; (C) single phase disordered perovskite.

matrix phase, BEI can detect much smaller amount of the secondary phase than XRD by their high spatial resolution (e.g.,  $\geq 0.01 \mu\text{m}$ ). Results of phase identification by XRD and of quantitative analysis using Rietveld analysis have been described in the previous work.<sup>7</sup> BEI of our samples consisted of three regions as follows: the matrix phase (BZT), the secondary phase and the pore. The secondary phases detected by XRD were found to be distinguished apparently from matrix phases by BEI observation also. From BEI, the contents of the secondary phases which were detected by XRD at (1)  $x=0.97$ , (2)  $y=0.97$  and (3)  $z=1.03$  were estimated to be about 6.7, 2.5 and 4.0%, respectively. In addition, a small amount of the secondary phases were found even in the samples which were not detected by XRD for (2)  $y=1.01$  and (3)  $z=1.00$  (BZT). The contents of the secondary phases were estimated to be about 0.2 and 0.8%, respectively. These results suggest that XRD is not able to detect the secondary phases less than 1%. By means of both BEI and XRD, the single phase ordered perovskite was found only in the composition of (1)  $x=1.01$  in this study. The single phase ordered perovskite was found in slightly Ba-rich and Zn-poor region in nominal composition rather than the stoichiometric BZT. However, a small composition deviation in the synthesis process cannot be ignored. We cannot determine the exact chemical composition of the single phase ordered perovskite. This has to be discussed with precise composition analysis. By quantitative composition analysis using XMA, the secondary phases were found to be a solid solution of  $\text{BaTa}_2\text{O}_6$  with certain amount of Zn. In contrast to the samples in the ordered perovskite region, the secondary phase was not observed in the samples in the disordered perovskite region by BEI observation also. By the BEI analysis, crystal structural phase diagram as shown in previous work<sup>7</sup> by XRD should be corrected more accurately. The revised crystal structural phase diagram is shown in Fig. 2. The crystal structural phases of BZT are distinguished into three parts as follows: (I) single phase ordered perovskite (vicinity of the stoichiometric BZT), (II) ordered perovskite with the secondary phase (Ta-

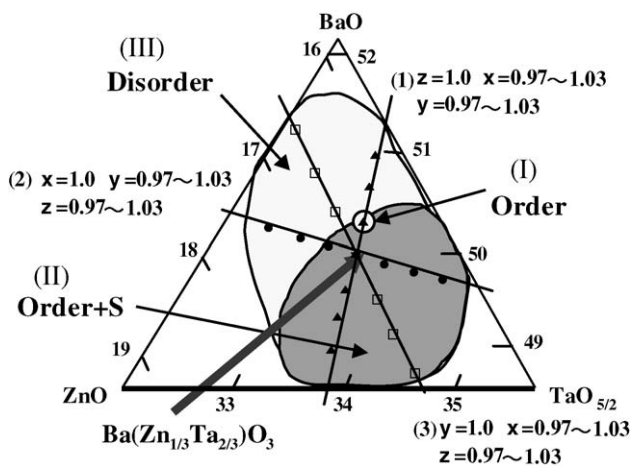


Fig. 2. Partial ternary phase diagram around BZT in  $x\text{BaO}-y(1/3\text{ZnO})-z(2/3\text{TaO}_{5/2})$  ( $x+y+z=3.0$ ). S shows the presence of secondary phase detected by BEI. Order: ordered perovskite (trigonal); Disorder: disordered perovskite (cubic).

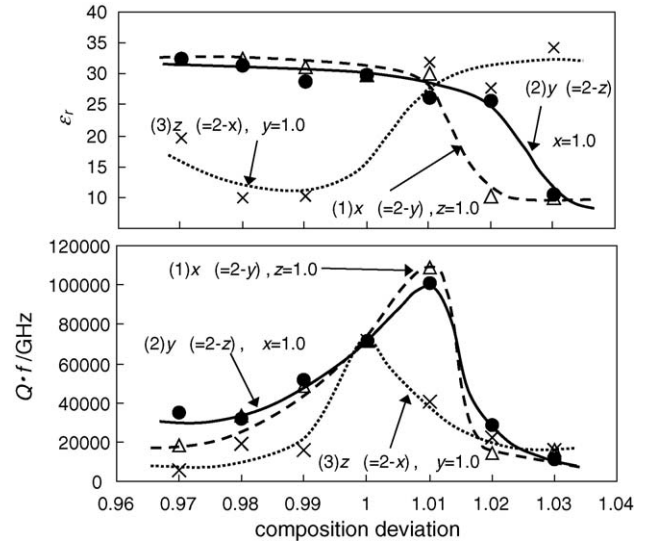


Fig. 3. Microwave dielectric properties dependence of composition deviation around BZT in  $x\text{BaO}-y(1/3\text{ZnO})-z(2/3\text{TaO}_{5/2})$  ( $x+y+z=3.0$ ) sintered at  $1400^\circ\text{C}$ .

rich region) and (III) disordered perovskite (Ba-rich or Ta-poor region).

### 3.2. The $Q \times f$ improvement limit of the single phase ordered BZT system

The composition dependence of microwave dielectric properties of ceramics has been shown in Ref. <sup>7</sup>. That is shown here in Fig. 3.  $\epsilon_r$  and  $Q \times f$  showed large variation depending on their composition. The stoichiometric BZT ( $x=y=z=1.00$ ) shows  $\epsilon_r=29.7$ ,  $Q \times f=71,360$  GHz. The maximum  $Q \times f$  value ( $\approx 108,600$ ,  $101,007$  GHz) was obtained at (1)  $x=1.01$  and (2)  $y=1.01$  slightly deviated from stoichiometric BZT with  $\epsilon_r$  value of 29.7 and 30.0, respectively. Fig. 4 shows the relationship between the ordering ratio and  $Q \times f$ . Even in the dense

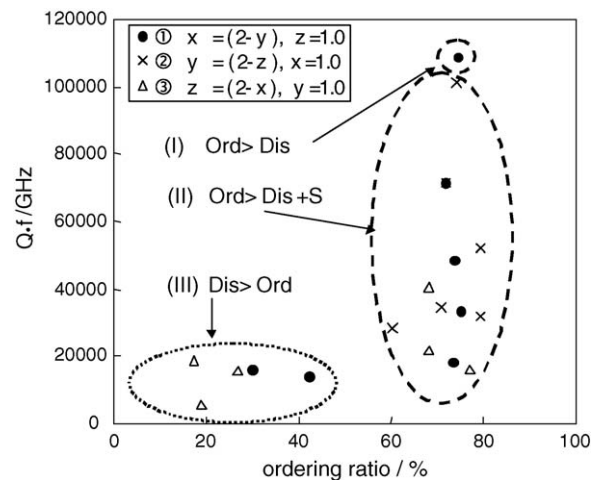


Fig. 4.  $Q \times f$  vs. ordering ratio on composition deviation around BZT in  $x\text{BaO}-y(1/3\text{ZnO})-z(2/3\text{TaO}_{5/2})$  ( $x+y+z=3.0$ ). S shows the presence of secondary phase detected by BEI. Ord: ordered perovskite (trigonal); Dis: disordered perovskite (cubic).

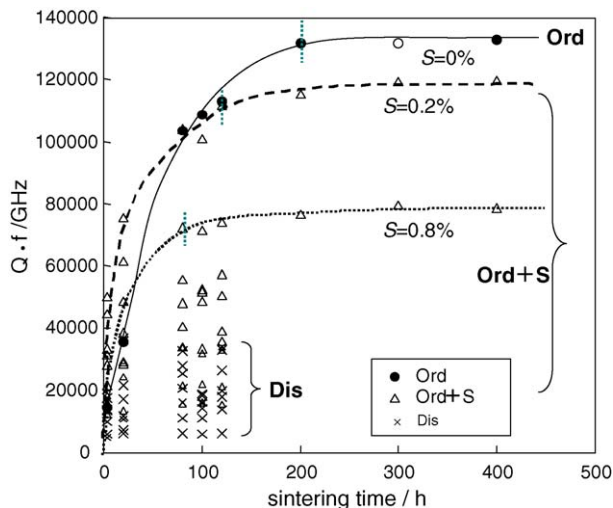


Fig. 5.  $Q \times f$  dependence of composition deviation around BZT in  $x\text{BaO}-y(1/3\text{ZnO})-z(2/3\text{TaO}_{5/2})$  as a function of sintering time at  $1400^\circ\text{C}$  ( $x+y+z=3.0$ ). S shows the contents of secondary phase detected by BEI. Ord: ordered perovskite; Dis: disordered perovskite; S: secondary phase.

(density =  $7.15\text{--}7.78\text{ g/cm}^3$ ), highly ordered region (estimated ordering ratio around 70–80%),  $Q \times f$  showed large variation ( $\approx 20,000\text{--}110,000\text{ GHz}$ ). The samples containing small amount of secondary phase detected by BEI in the highly ordered perovskite region showed relatively lower value of the  $Q \times f$  in comparison to samples without secondary phase. This result indicates that decrease of  $Q \times f$  in the highly ordered samples can attribute to the presence of the secondary phase. Therefore, the maximum  $Q \times f$  value ( $=108,600\text{ GHz}$ ) was obtained in single phase ordered perovskite at (1)  $x=1.01$ .

To find out the  $Q \times f$  improvement limit of the single phase ordered perovskite, we performed extended sintering duration up to 400 h at  $1400^\circ\text{C}$  using several samples with high  $Q \times f$  value for comparison. The results are shown in Fig. 5. The  $Q \times f$  of the single phase ordered perovskite continued to improve with sintering time up to 200 h and reached the maximum value of 133,000 GHz. Then, the  $Q \times f$  showed saturation for sintering duration exceeding 200 h. On the other hand, samples with the secondary phase, the  $Q \times f$  improvement saturated with a lower  $Q \times f$  value and at shorter sintering time than that of the single phase ordered perovskite. This saturation in sintering time seems to depend on the amount of the secondary phase in the samples. For example, the contents of the secondary phase were 0, 0.2 and 0.8%, and the corresponding saturation points were about 200, 120 and 80 h, respectively.

## 4. Conclusions

Influences of composition deviation from the stoichiometric BZT on the structural order and the  $Q$  factor were studied. Our findings are listed below. (1) The crystal structure phases strongly depend on the slight composition deviation from the stoichiometric BZT. (2) Single phase ordered perovskite was obtained only in the vicinity of the stoichiometric BZT. In this region, an improvement in  $Q$  factor ( $Q \times f = 133,000\text{ GHz}$ ) was found in extended sintering up to 400 h at  $1400^\circ\text{C}$ . (3) In the other regions, the single phase of the disordered perovskite or the ordered perovskite with the secondary phase were formed. In these regions the  $Q$  factor was found to be low. (4) Presence of small amount of secondary phase (e.g., less than 1%) affects  $Q$  factor decrements. This suggests that the structural order and the presence of the secondary phase were playing an important role on  $Q$  factor in the BZT system. Therefore, suppressions of small amount of secondary phase (e.g., less than 1%) and increase of ordering ratio by strict composition control can provide further  $Q$  factor improvements in the BZT system.

## References

1. Wakino, K., Recent development of dielectric resonator materials and filters in Japan. *Ferroelectrics*, 1986, **91**, 69–86.
2. Kawashima, S., Nishida, M., Ueda, I. and Ouchi, H.,  $\text{Ba}(\text{Zn}_{1/3}\text{Ta}_{2/3})\text{O}_3$  ceramics with low dielectric loss at microwave frequencies. *J. Am. Ceram. Soc.*, 1983, **66**, 421–423.
3. Gallasso, F. and Darby, W., Ordering in compounds of the  $\text{A}(\text{B}_{0.33}\text{Ta}_{0.67})\text{O}_3$  type. *Inorg. Chem.*, 1963, **2**(3), 482–484.
4. Sagala, D. A. and Nambu, S., Microscopic calculation of dielectric loss at microwave frequencies for  $\text{Ba}(\text{Zn}_{1/3}\text{Ta}_{2/3})\text{O}_3$ . *J. Am. Ceram. Soc.*, 1992, **75**, 2573–2575.
5. Tamura, H., Three-dimensional dielectric dispersion equation for Zn–Ta–Ta system in  $\text{Ba}(\text{Zn}_{1/3}\text{Ta}_{2/3})\text{O}_3$  crystal. *Jpn. J. Appl. Phys.*, 1993, **32**, 2774–2779.
6. Koga, E. and Moriwake, H., Effects of superlattice ordering and ceramic microstructure on the microwave  $Q$  factor of complex perovskite-type oxide  $\text{Ba}(\text{Zn}_{1/3}\text{Ta}_{2/3})\text{O}_3$ . *J. Ceram. Soc. Jpn.*, 2003, **111**, 767–775 (in Japanese).
7. Koga, E., Moriwake, H., Kakimoto, K. and Ohsato, H., Influences of composition deviation from stoichiometric  $\text{Ba}(\text{Zn}_{1/3}\text{Ta}_{2/3})\text{O}_3$  on superlattice ordering and microwave quality factor  $Q$ . *J. Ceram. Soc. Jpn.*, 2005, **113**, 172–178 (in Japanese).
8. Izumi, F. and Ikeda, T., A Rietveld-analysis program RIETAN-98 and its applications to zeolites. *Mater. Sci. Forum*, 2000, **198**, 321–324.
9. Hakki, B. W. and Coleman, P. D., A dielectric method of measuring inductive capacities in the millimeter range. *IEEE Trans. Microwave Theory Tech.*, 1980, **MTT-8**, 402–440.